

ADAPTIVE GALLAGER CODED MODULATION SCHEME ON RAYLEIGH FADING CHANNELS: COMPARISON OF SIMULATED AND THEORETICAL PERFORMANCE

Ola Jetlund, Geir E. Øien, Kjell J. Hole, and Bengt Holter

Department of Telecommunications, Norwegian University of Science and Technology,
N-7491 Trophism, NORWAY

ABSTRACT

Adaptive coding and modulation (ACM) is a promising technique designed to combat fading on a mobile radio channel. An ACM scheme adapts spectral efficiency to the temporal variations in the fading envelope. In this paper we present results from computer simulations of a complete transmission system using ACM. Our ACM scheme employs pilot symbol assisted modulation in order to provide information about the fading at the receiver. This information is used in both channel estimation and in channel prediction, which enables adaptivity. The simulated performance in terms of spectral efficiency and bit error rate is compared to theoretical measures.

1. INTRODUCTION

Traditional wireless communication systems use a single channel code and a single modulation constellation (“codec”) to combat the impairments introduced by a *multipath fading channel* (MFC). When the *channel signal-to-noise ratio* (CSNR) is above a certain level, γ_1 , transmission is done using this codec. When the CSNR is below γ_1 , the codec used can not guarantee a specified quality, and the system experiences an *outage*. These traditional systems (e.g. GSM) are designed to function at almost all locations within a given distance from a base station. Thus, in order to keep the outage probability acceptably low, γ_1 must be sufficiently low. This comes at the expense of a low *spectral efficiency* (SE), defined as the number of information bits transmitted per second per unit available bandwidth ([bits/s/Hz]).

An *adaptive coding and modulation* (ACM) scheme on the other hand, is used to combat the impairments introduced by a *frequency-flat* MFC such that the *average SE* (ASE) is maximized for the range of possible CSNR values on the MFC, while still providing a *bit error rate* (BER) below a certain *target bit error rate*, BER_0 . ACM systems employ multiple codecs in order to adapt the SE to the variations in the CSNR. Theoretical performance analysis has

previously been performed for such systems, assuming certain idealized conditions. ACM can be applied to frequency-selective channels when each subchannel in a multicarrier—e.g. an orthogonal frequency division multiplexing—scheme [1], experiences flat fading [2]. In ACM both the transmitter and receiver need to have knowledge about the channel quality (the *channel state information* (CSI)). This is achieved by transmitting the CSI from the receiver to the transmitter on a separate return channel. The CSI must be predicted for future transmissions at the receiver based on information on the fading process extracted from received channel symbols. The performance of an ACM system depends on several factors: the degree of mobility (terminal velocity), the prediction filter order, available information about the fading process at the receiver, delay and errors in the return channel.

In this paper we present results from computer simulations of a complete ACM system on a Rayleigh fading channel. The simulated system uses *pilot symbol assisted modulation* (PSAM) [3] to provide the receiver and the transmitter with information on the fading envelope. The goal of this paper is to confirm previous theoretical analysis by means of simulations. Also, we want to ascertain under which practical conditions the assumptions used during analysis actually hold.

2. CHANNEL MODEL

A signal transmitted on a mobile radio channel is scattered, reflected, and diffracted by objects in the radio environment [1], resulting in an MFC. The MFC is time varying due to the transmitter, the receiver, and obstructing objects moving in different directions and at different velocities. The fading channel is *frequency-flat* if all frequency components of a transmitted signal are affected by the same channel gain. In a complex baseband model of a flat MFC the received signal at time t can be written as $y(t) = z(t) \cdot x(t) + n(t)$, where $x(t)$ is the transmitted complex-valued symbol, $n(t)$ is complex-valued *additive white gaussian noise* (AWGN), and $z(t)$ is the complex fading gain. The

fading is assumed to be a wide-sense stationary (WSS) process. Then the instantaneous received CSNR is defined as

$$\gamma(t) = \frac{|z(t)|^2 \cdot P}{N_0 B}, \quad (1)$$

with expectation

$$E[\gamma(t)] = \bar{\gamma} = \frac{\Omega_p \cdot P}{N_0 B}, \quad (2)$$

where P [W] is the average transmit power, N_0 [W/Hz] is the noise power spectral density, B [Hz] is the transmission bandwidth, and $\Omega_p = E[|z(t)|^2]$ is the average power gain.

We shall assume that the magnitude of the received complex fading envelope $\alpha(t) = |z(t)|$ has a Rayleigh distribution [1]. Then the squared envelope $\alpha^2(t)$ has an exponential distribution.

A WSS MFC can be characterized by its maximum Doppler frequency, f_m [Hz], given by $f_m = \frac{v}{c} f_c$, where v [m/s] is the velocity of the relative transmitter-receiver motion, c [m/s] is the speed of light, and f_c [Hz] is the carrier frequency. Under the assumption of isotropic scattering, the fading is said to have a Jakes spectrum, and the autocorrelation of the complex fading envelope can be written as [1, pp. 44-46]

$$\phi_{zz}(\tau) = \frac{1}{2} E[z^*(t)z(t+\tau)] = \frac{\Omega_p}{2} J_0(2\pi f_m \tau), \quad (3)$$

where $J_0(\cdot)$ is the *zero-order Bessel function of the first kind*, and τ is the time delay between samples. The higher v , and thus f_m , the less correlated the fading typically is for a given τ .

3. THE ADAPTIVE CODED MODULATION SCHEME

Our ACM system was originally presented in [4, 5, 6]. Channel codes from the very promising class of block codes called Gallager codes (or *low-density parity check* codes) [7], are used as component codes. Coded information is modulated using gray mapping and a QAM or a PSK constellation (parameters describing simulated codecs are shown in Table 1).

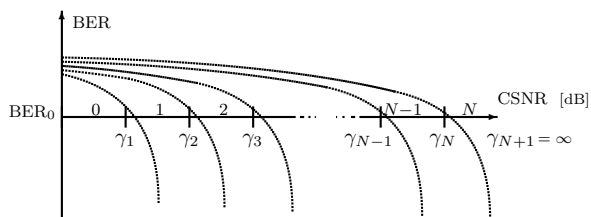


Figure 1: Fading regions.

The ACM scheme employs N different codecs, indexed by $n \in \{1, 2, \dots, N\}$, designed for AWGN channels at different CSNRs. The range of possible CSNR values on the MFC, $\gamma \in [0, \infty)$, is divided into $N + 1$ fading regions. The CSNR falls into fading region n when $\gamma_n \leq \gamma < \gamma_{n+1}$. The predicted CSNR is denoted $\hat{\gamma}$, thus the system experiences an outage when $\hat{\gamma} \in [0, \gamma_1)$. Otherwise codec n should be assigned when $\hat{\gamma} \in [\gamma_n, \gamma_{n+1})$. Here we assume $\gamma_{N+1} = \infty$. The corresponding SE is denoted R_n [bits/s/Hz], and it is assumed that $R_1 < R_2 < \dots < R_N$.

The thresholds $\gamma_1, \gamma_2, \dots, \gamma_N$ are based on the BER performance for each of the codecs. Each codec is simulated on AWGN channels to obtain the relationship between BER and CSNR. The threshold for a given codec is then found by curve fitting on the simulated BER data and selecting the CSNR range for each codec such that $\text{BER} \leq \text{BER}_0$ (we refer to [5] for details). This is illustrated in Figure 1.

The CSI, the selected fading region, is obtained by channel prediction. The optimal predictor implemented in our simulations is described in the following section. After the prediction the fading region index n is transmitted from the receiver to the transmitter (see Figure (2)). The return channel is assumed free of errors, but with a transmission delay known at the receiver. When the CSI information changes, the transmitter and receiver adapt, that is, perform a codec update, in order to maximize the SE.

The ASE of an ACM transmission scheme is used as a performance measure. The ASE is equal to $\text{ASE} = \sum_{n=1}^N R_n \cdot P_n$ [bits/s/Hz], where P_n is the probability of codec n being used, and can be found from the probability distribution of the fading [8]. We will simulate the ASE by time-averaging the experienced SEs of the system for each given average CSNR. A more detailed description of both the ACM scheme, and the Gallager codes used, is available in [5].

4. PILOT SYMBOL ASSISTED MODULATION

PSAM is a technique designed to provide the receiver with information on the fading envelope, in order to perform channel estimation and coherent detection [3, 9]. In PSAM deterministic pilot symbols are periodically inserted into the stream of information carrying channel symbols to be transmitted. When PSAM is used the complex fading envelope $z(t)$ can be esti-

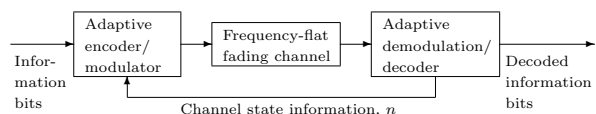


Figure 2: Transmission System.

mated at any time t independent of any decisions done in the past [9]. The pilot positions must be known at both the transmitter and the receiver. In the following subsections we describe the use of PSAM in channel estimation and prediction of the CSI.

4.1. Channel Estimation

Introducing discrete time indexing, the received signal can be written as $y(k) = z(k) \cdot x(k) + n(k)$, where $x(k)$ is the information signal except at the pilot instants $k = lL$ where l is an integer and L is a constant integer larger than zero. Although we do not claim that this is optimal, we shall assume that all pilot symbols have the same value $x(lL) = a_p$, and that the power for pilots and information symbols is equal, that is, $|a_p| = \sqrt{P}$.

At each pilot symbol instant lL , the following *maximum likelihood* (ML) estimate (based on one received observation [9, Equation (14-35)]) of $z(lL)$ is calculated by the receiver: $\tilde{z}(lL) = \frac{y(lL)}{a_p} = z(lL) + \frac{n(lL)}{a_p}$. The ML estimates are shifted into a buffer of size K_e , where K_e is an even integer. The buffered estimates, at time instant k ,

$$\tilde{\mathbf{z}}_k = [\tilde{z}(k), \tilde{z}(k-L), \dots, \tilde{z}(k-(K_e-1)L)]^T, \quad (4)$$

where $k = lL$, can then be used to estimate $z(k-j)$ by a linear interpolation filter of order K_e . The estimated value can be written as (see e.g. [9]) $\hat{z}(k-j) = \mathbf{h}_j^T \tilde{\mathbf{z}}_k$, where

$$\mathbf{h}_j = [h_j(0), h_j(1), \dots, h_j(K_e-1)]^T, \quad (5)$$

is the vector holding the estimation filter coefficients which correspond to estimating the symbol at time instant $k-j$. The filter uses $K_e/2$ ML estimates in the future and $K_e/2$ ML estimates in the past to perform one fading estimate. That is, at time instant k the receiver estimates the fading at time instant $k-j$, $j \in \{(K_e/2-1)L+1, (K_e/2-1)L+2, \dots, (K_e/2)L-1\}$. A side effect of this technique is that it introduces a delay at the receiver.

From [2, Equation (5)], the *maximum a posteriori* (MAP) optimal filter coefficient vector on a Rayleigh fading channel is

$$\mathbf{h}_{j,\text{MAP}} = \mathbf{r}_{j,K}^T \left(\mathbf{R}_K + \frac{1}{\gamma} \mathbf{I}_{K \times K} \right)^{-1}, \quad (6)$$

with $K = K_e$, where $\mathbf{r}_{j,K}$ is a vector with K elements representing the covariance between the fading to be estimated at time $k-j$ and the fading at the pilot instants $k, k-L, k-2L, \dots, k-(K-1)L$, and \mathbf{R}_K is a $K \times K$ -matrix holding the autocorrelation of the fading process sampled at a period equal $L \cdot T_s$, where T_s is the duration of a single channel symbol. With

the assumption of Jakes spectrum in the fading process, the elements of $\mathbf{r}_{j,K}$ and \mathbf{R}_K can be calculated from the following equations [2, 10] (using the autocorrelation in Equation (3)):

$$[\mathbf{r}_{j,K}]_l = \frac{2}{\Omega_p} \phi_{zz}((j+lL)T_s), \quad (7)$$

and

$$[\mathbf{R}]_{lm} = \frac{2}{\Omega_p} \phi_{zz}(|l-m|LT_s), \quad (8)$$

where l and m are integers.

4.2. Channel prediction

Channel prediction is done using K_p ML-estimates in the past to predict the CSNR at the j th symbol *ahead in time*. That is, the MAP-optimal *prediction* filter coefficients, $\mathbf{h}_{j,\text{MAP}}$, is calculated from Equation (6) with $K = K_p$. We define $\hat{\alpha} = |\hat{z}|$ with corresponding $E[\hat{\alpha}^2] = \hat{\Omega}_p$, and then there exists a constant r such that $\hat{\Omega}_p = r \cdot \Omega_p$ [2, 10]. Since the predicted fading envelope is a linear combination of complex gaussians, it is itself a complex gaussian. It follows that the $\hat{\alpha}$ is Rayleigh distributed, and that the corresponding predicted CSNR,

$$\hat{\gamma}(k) = \frac{|\hat{\alpha}(k)|^2 P}{N_0 B}, \quad (9)$$

is exponentially distributed with expectation

$$E[\hat{\gamma}] = \frac{\hat{\Omega}_p P}{N_0 B} = r \cdot \gamma. \quad (10)$$

The correlation coefficient between predicted CSNR and actual CSNR is defined as

$$\rho = \frac{\text{Cov}(\hat{\gamma}, \gamma)}{\sqrt{\text{Var}(\hat{\gamma}) \text{Var}(\gamma)}}, \quad (11)$$

where $\text{Cov}(\cdot, \cdot)$ denotes the *covariance* and $\text{Var}(\cdot)$ denotes *variance*. It is shown in [10] that for the MAP-optimal predictor, the ratio r and the correlation coefficient ρ are both equal to

$$\rho = r = \mathbf{r}_{j,K}^T \left(\mathbf{R}_K + \frac{1}{\gamma} \mathbf{I}_{K \times K} \right)^{-1} \mathbf{r}_{j,K}, \quad (12)$$

with $K = K_p$.

The receiver predicts the future CSI after each received block of channel symbols, and the delay between the receiver prediction and the transmitter update is referred to as the *prediction lag*. Because of the block structure of the Gallager codes employed by the ACM scheme, it is only feasible to update the codec used between two successive transmitted blocks. Thus, an underlying assumption—during system analysis—is that the fading is slow enough to

stay within the same fading region over one transmitted block. The channel symbol block length after pilot insertion is denoted M' , and is equal to $M(\frac{L+1}{L})$, where M is the number of channel symbols corresponding to one codeword. The prediction lag is $j \in \{0, M', 2M', \dots\}$. Introducing pilots into the transmitted block thus reduces the SE of one block by the factor $M/M' = \frac{L}{L+1}$ and the resulting ASE becomes $\text{ASE} = \frac{M}{M'} \sum_{n=1}^N R_n \cdot P_n$ [bits/s/Hz].

5. SIMULATIONS

5.1. System overview

Our simulation software simulates the transmission system in Figure 2. The information bits input to the encoder come from a random bit stream with a uniform distribution. For each information block, the information bits are coded and modulated using the codec selected by the CSI index n on the return channel. The code rate, constellation size, SE, and CSNR thresholds of each of the $N = 5$ codecs in our software are shown in Table 1. Note that the SE of codec n equals the codec number, that is, $R_n = n$.

The results presented here use $M = 200$ symbols/block and $L = 10$, resulting in an $M' = 220$. The CSNR thresholds for the 5 codecs in Table 1 were simulated using $\text{BER}_0 = 10^{-3}$ in [5].

In [6] we implemented a Rayleigh fading simulator with the autocorrelation in Equation (3), based on the work by Smith [11] and Young and Beaulieu [12]. The simulator produces samples of the Rayleigh fading envelope and the AWGN. The carrier frequency in our simulation setup is $f_c = 5.4$ GHz, the symbol duration is $T_s = 4 \mu\text{s}$, the average power gain is set to $\Omega_p = 1$, the transmit power is $P = 1$ W, and the variance of the AWGN $\sigma_w^2 = N_0 B$ is varied such that the expected CSNR (in dB) is $\bar{\gamma} \in [0, 25]$ [dB].

At the receiver, the channel symbols at the pilot positions are collected from the received block, and are used both in the prediction [2, 10] and estimation [3]. For further information on the demodulator and decoder we refer to [5, 6].

Codec $n = R_n$	Code rate	Constellation size and type	Threshold γ_n [dB]
1	1/2	4QAM	2.72
2	2/3	8PSK	8.03
3	3/4	16QAM	11.21
4	4/5	32QAM	14.91
5	5/6	64QAM	17.89

Table 1: SE, code rate, corresponding constellation, and thresholds, for $\text{BER}_0 = 10^{-3}$, for the 5 codecs employed by the ACM system.

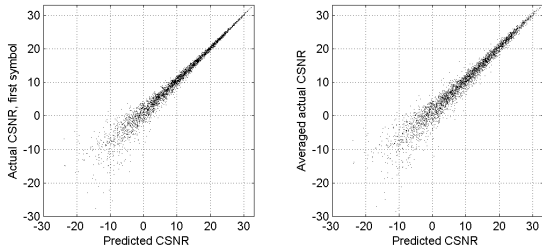


Figure 3: Scatter plot of predicted versus actual CSNR (leftmost plot) and averaged actual CSNR (rightmost plot) for $v = 5$ m/s and $j = 1 \cdot M'$.

The result from the ML estimator is shifted into a buffer, which in our simulations is chosen to be of size $K_e = 3000$. The predictor filter order is chosen to be $K_p = K_e/2$. This is not intended as practically feasible predictor or estimator order, but are chosen as approximations of $K_e = \infty$ and $K_p = \infty$ (corresponding to the lowest possible mean square error). For each received block of channel symbols $[z(lL), z(lL+1), \dots, z(lL+M'-1)]$, the channel predictor uses the filter described in Section 4, to calculate $\hat{z}(lL+jM')$, that is, the predicted fading of the first symbol in the block of channel symbols to be transmitted j block lengths ahead. The system assumes that the fading is approximately constant during transmission of one block, and that this prediction can therefore be used for an entire block of size M' . Using Equation (10) the predicted CSNR is found and the codec index n is chosen such that $\gamma_n \leq \hat{\gamma} < \gamma_{n+1}$, using the thresholds in Table 1. The index n is transmitted back to the transmitter on a separate, zero-error return channel. The prediction lag j is varied to allow for both computational delays in the receiver and for a transmission delay in the return channel.

5.2. Predictor performance

In the leftmost plot in Figure 3 a scatter plot of outcomes of the predicted CSNR versus the actual CSNR ($\hat{\gamma}(k)$ versus $\gamma(k)$) is shown. The scatter plots show 100 simulated points per $\bar{\gamma} \in \{0, 1, 2, \dots, 25\}$ [dB]. The experiment was replicated in the rightmost plot for the predicted CSNR versus the empirical blockwise average of the CSNR for the entire block of channel symbols ($\hat{\gamma}(k)$ versus $\bar{\gamma}_{M'}(k)$),

$$\bar{\gamma}_{M'}(k) = \frac{1}{M'} \sum_{l=k}^{k+M'} \gamma(l). \quad (13)$$

In both plots, the velocity and the prediction lag was set to $v = 5$ m/s and $j = M'$ respectively.

Perfect prediction would yield $\hat{\gamma}(k) = \gamma(k)$, thus all points in the scatter plots showing $\hat{\gamma}(k)$ versus $\gamma(k)$ would be located on a *reference line* with a positive

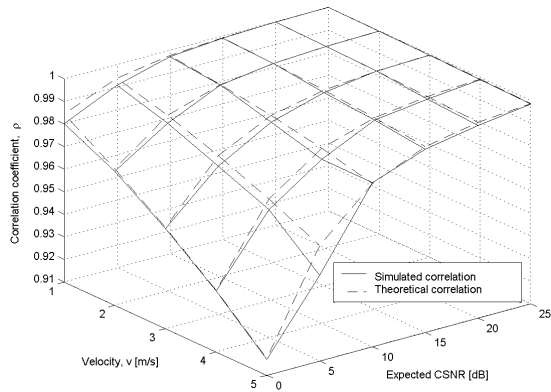


Figure 4: The correlation coefficient as a function of velocity v and expected CSNR $\bar{\gamma}$ for $j = M'$.

slope equal to one (going through the point $(0,0)$). In addition, if the fading were constant during transmission of a block of channel symbols, the points in the scatter plots showing $\hat{\gamma}(k)$ versus $\bar{\gamma}_{M'}(k)$ would be located on the reference line with slope one.

As we could expect, the largest prediction errors occur at the deepest fades of the fading envelope. Comparing the $\hat{\gamma}(k)$ versus $\gamma(k)$, to the $\hat{\gamma}(k)$ versus $\bar{\gamma}_{M'}(k)$, we observe that the prediction error increases somewhat, although not dramatically. This is due to the fact that the fading is highly correlated (not far from constant over a block) due to the low velocities used. It can be observed that the prediction tends to be lower than the actual CSNR, that is, the predictor tends to underestimate the CSNR.

The correlation coefficient ρ between the predicted CSNR and actual CSNR is plotted against average expected CSNR and velocity in Figure 4. The theoretical correlation is plotted for reference. The figure shows how ρ increases as $\bar{\gamma}$ increases and how ρ is reduced when velocity increases (or equivalently the correlation of the fading envelope decreases). The simulated correlation coefficient is smaller than or equal to the theoretical correlation in Equation (12). From this and Equation (10), we would expect that the predicted CSNR is lower than the actual CSNR, as was also observed from the scatter plots. Thus, we would expect a good BER performance, but a reduced ASE.

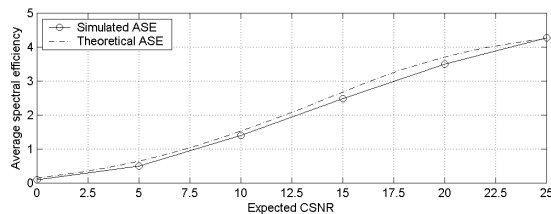


Figure 5: Simulated ASE plotted against expected CSNR for $v = 1$ m/s, and $j = 1 \cdot M'$.

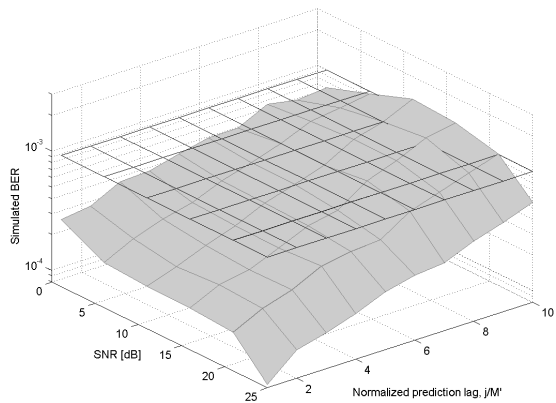


Figure 6: BER plotted against expected CSNR and varying prediction lags, and $v = 1$ m/s. The plane at $BER_0 = 10^{-3}$ is plotted for evaluation, that is, points on the BER curve below the plane satisfy the BER demand.

5.3. ACM performance

Both the BER and ASE are performance measures for the ACM scheme. In Figure 5 simulated ASE is plotted against $\bar{\gamma} \in [0, 25]$ dB for $v = 1$ m/s, and a prediction lag $j = M'$. The theoretical ASE is plotted for comparison. We see from the figure that the simulated ASE is lower than the theoretical ASE, that is, the predictor tends to underestimate the CSNR.

Figure 6 and 7 show surface plots of the BER as a function of CSNR, and prediction lag and velocity respectively. A plane at BER_0 is added for reference. In Figure 6, the velocity is $v = 1$ m/s. The figure shows that the BER performance is reduced for increasing j , and that for all prediction lags $j \leq 8 \cdot M'$, the BER demand of BER_0 is satisfied. Figure 7 shows that the BER increases with increasing velocity, and the BER demand is only satisfied $v < 2$ m/s unless the expected CSNR is relatively high ($\bar{\gamma} > 13$ dB), where the demand is also satisfied for $v = 3$ m/s. From both figures it can be observed that the BER performance improves with increased expected CSNR, except for the case when the prediction lag is high ($j > 6 \cdot M'$), where the BER increases up to a $\bar{\gamma} \simeq 15$ [dB]. The poor BER performance at high prediction lags might be explained by some of the Gallager codes (at medium CSNRs) being very sensitive to prediction errors caused by high prediction lags.

6. CONCLUDING REMARKS

Prediction errors cause degradation in the BER performance of the ACM scheme when $\hat{\gamma}(k) > \gamma(k)$. In our system we predict the CSNR for the first symbol in a block of M' symbols. The system assumes that the CSNR is approximately constant during trans-

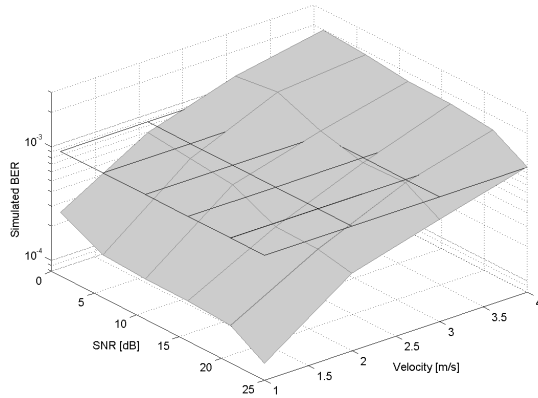


Figure 7: BER plotted against expected CSNR and varying velocities, and $j = M'$. The plane at $\text{BER}_0 = 10^{-3}$ is plotted for evaluation, that is, points on the BER curve below the plane satisfy the BER demand.

mission of one block, and uses the prediction to select a region for an entire block. Since the fading is time varying also within one block, the instantaneous CSNR may fall below the threshold during the block transmission.

From the scatter plots we see that the prediction error is largest when the actual CSNR is low. Points located below the reference line indicates that $\hat{\gamma}(k) > \gamma(k)$, which is likely to lead to a $\text{BER} > \text{BER}_0$. By comparing the scatter plots for $\hat{\gamma}(k)$ versus $\gamma(k)$ to the $\hat{\gamma}(k)$ versus $\bar{\gamma}_{M'}(k)$, we observe that the assumption of approximately constant fading during transmission of a block of channel symbols is slightly optimistic, but still quite accurate for the simulations presented here.

To sum up, the results in Figure 6 and Figure 7 indicate that increasing velocity and/or increasing the time delay may reduce the BER performance such that $\text{BER} > \text{BER}_0$. Furthermore the BER performance of the ACM scheme will improve by increasing the expected CSNR.

A possible way of improving BER performance which would not reduce the ASE might be to include an interleaver. But as indicated by the results in [13], the BER performance of a Gallager code on a correlated Rayleigh fading channel yields only very small improvements by introducing an interleaver.

7. REFERENCES

- [1] G. L. Stüber, *Principles of Mobile Communication*. Kluwer Academic Publishers, 2nd ed., 2001.
- [2] G. E. Øien, H. Holm, and K. J. Hole, "Channel prediction for adaptive coded modulation in Rayleigh fading," in *Proc. European Signal Processing Conference (EUSIPCO)*, (Toulouse, France), Sept. 2002.
- [3] J. K. Cavers, "An analysis of pilot symbol assisted modulation for Rayleigh fading channels,"

IEEE Transactions on Vehicular Technology, vol. 40, pp. 686–693, November 1991.

- [4] B. Myhre, V. Markhus, and G. E. Øien, "LDPC coded adaptive multilevel modulation for slowly varying Rayleigh-fading channels," in *Proc. NORSIG*, (Trondheim, Norway), pp. 129–134, Oct. 2001.
- [5] O. Jetlund, G. E. Øien, K. J. Hole, V. Markhus, and B. Myhre, "Rate-adaptive coding and modulation with LDPC component codes," Technical Document TD(02) 108, Cooperation européenne dans le domaine de la recherche Scientifique et Technique - 273 (02), Lisbon, Portugal, September 2002.
- [6] O. Jetlund, G. E. Øien, and K. J. Hole, "Adaptive Gallager coded modulation on Rayleigh fading channels: Comparison of simulated and theoretical performance," Technical Document TD(03) 040, Cooperation européenne dans le domaine de la recherche Scientifique et Technique - 273 (03), Barcelona, Spain, January 2003.
- [7] R. G. Gallager, *Low-Density Parity-Check Codes*. Cambridge, Massachusetts: M.I.T. Press, 1963.
- [8] A. J. Goldsmith and S.-G. Chua, "Variable-rate variable-power MQAM for fading channels," *IEEE Transactions on Communications*, vol. 45, pp. 1218–1230, Oct 1997.
- [9] H. Meyr, M. Moeneclaey, and S. A. Fechtel, *Digital Communication Receivers*. John Wiley & Sons, Inc, 1998.
- [10] G. E. Øien, H. Holm, and K. J. Hole, "Adaptive coded modulation enhanced by channel prediction and antenna diversity," Technical Document TD(02) 054, Cooperation européenne dans le domaine de la recherche Scientifique et Technique - 273 (02), Espoo, Finland, May 2002.
- [11] J. I. Smith, "A computer generated multipath fading simulation for mobile radio," *IEEE Transactions on Vehicular Technology*, vol. VT-24, pp. 39–40, August 1975.
- [12] D. J. Young and N. C. Beaulieu, "The generation of correlated Rayleigh random variates by inverse discrete Fourier transform," *IEEE Transactions on Communications*, vol. 48, pp. 1114–1127, July 2000.
- [13] S. Guo, S. Ng, and L. Hanzo, "LDPC assisted block coded modulation for transmission over Rayleigh fading channels," in *Proc. Vehicular Technology Conference, 2003, IEEE 57th*, (JEJU, Korea), April 2003.

References [5, 6, 10] are available at <http://www.tele.ntnu.no/projects/beats>.